

# Wood Particle/High-Density Polyethylene Composites: Thermal Sensitivity and Nucleating Ability of Wood Particles

Hassine Bouafif,<sup>1</sup> Ahmed Koubaa,<sup>1</sup> Patrick Perré,<sup>2</sup> Alain Cloutier,<sup>3</sup> Bernard Riedl<sup>3</sup>

<sup>1</sup>Chaire de Recherche du Canada sur la Valorisation, la Caractérisation et la Transformation du Bois, Université du Québec en Abitibi-Témiscamingue, 445 BD de l'Université, Rouyn-Noranda, Québec, Canada J9X5E4

<sup>2</sup>AgroParisTech, Institut National de la Recherche Agronomique, Unite Mixte de Recherche 1093, Laboratoire d'Etudes et de Recherche sur le Matériau Bois, 14 Rue Girardet, Nancy, France 54000

<sup>3</sup>Centre de Recherche sur le Bois, Université Laval, Pavillon Gene-H.-Krugler, Québec, Québec, Canada G1V 0A6

Received 21 September 2008; accepted 28 January 2009

DOI 10.1002/app.30129

Published online 19 March 2009 in Wiley InterScience (www.interscience.wiley.com).

**ABSTRACT:** The thermal sensitivity, nucleating ability, and nonisothermal crystallization of high-density polyethylene (HDPE) with different wood fillers during wood/HDPE melt processing were investigated with thermogravimetric analysis and differential scanning calorimetry. The results showed that the wood degraded at a lower temperature than HDPE. The thermal decomposition behavior was similar across wood species. The most remarkable dissimilarities were observed between wood and bark in the decomposition rate around a processing temperature of 300°C and in the peak temperature location for cellulose degradation. The higher degradation rate for bark was explained by the devolatilization of extractives and the degradation of lignin, which were present in higher amounts in pine bark. The nucleating

ability for various wood fillers was evaluated with the crystalline weight fraction, crystal conversion, crystallization half-time, and crystallization temperature of the HDPE matrix. The nucleation activity improved with the addition of wood particles to the HDPE matrix. However, no effect of wood species on the crystal conversion was found. For composites based on semicrystalline matrix polymers, the crystal conversion may be an important factor in determining the stiffness and fracture behavior. © 2009 Wiley Periodicals, Inc. *J Appl Polym Sci* 113: 593–600, 2009

**Key words:** composites; differential scanning calorimetry (DSC); nucleation; thermogravimetric analysis (TGA); thermoplastics

## INTRODUCTION

A common and key limitation to the use of natural fibers in composites is thermal degradation. Knowledge of the appropriate and/or maximum processing temperature is therefore critical for the development of thermosetting and thermoplastic composites. It is known that thermal treatment leads to a variety of physical<sup>1</sup> and chemical<sup>2–5</sup> changes in wood. Christiansen<sup>6</sup> reported that overdrying wood reduces bonding to phenol–formaldehyde adhesives. He described three inactivation mechanisms involving physical responses to overdrying: (1) exudation of extractives to the surface, which lowers wettability by coating the surface; (2) reorientation of wood surface molecules, which reduces wettability, or

bonding sites; and (3) irreversible closure of large micropores in cell walls. Sernek et al.<sup>7</sup> attributed surface inactivation to the concentration of nonpolar substances, hydrophobic extractives, and volatile organic compounds on wood surfaces during the drying process at temperatures above 160°C.

Various analytical methods can be used to assess the thermal degradation of wood. Thermogravimetric analysis (TGA) and differential scanning calorimetry (DSC) are two useful methods. Thermal stability is difficult to assess because of the composite nature of wood, which is a mixture of hemicelluloses, cellulose, and lignin. Wood also contains extractives, which play a determinant role in the development of wood properties, despite their low concentration. Thermal degradation of natural fibers can be described as a two-stage process: the first stage in the temperature range of 220–280°C and the second stage in the range of 280–300°C. Hemicelluloses degrade in the low temperature range, and cellulose degrades in the high temperature range.<sup>8–10</sup> Ramiah<sup>8</sup> studied thermal degradation in different cellulose, hemicellulose, and lignin samples. Results calculated from static and dynamic TGA indicated that the

Correspondence to: H. Bouafif (hassine.bouafif@uqat.ca).

Contract grant sponsors: Canada Research Chair Program, Ministère du Développement Économique, Innovation et Exportation (Québec), Caisse Populaire Desjardins, Tembec, La Fondation de l'Université du Québec en Abitibi-Témiscamingue.

activation energy for thermal degradation for the three components was in the range of 151–251, 63–109, and 54–80 kJ/mol, respectively. Orfão et al.<sup>11</sup> investigated the thermogravimetric behavior of cellulose, xylan, and lignin in inert and oxidizing atmospheres. They concluded that the cellulose decomposition rates became measurable at about 225°C in both air and nitrogen, whereas xylan began decomposing at lower temperatures (160°C). However, fractions corresponding to the low-temperature decomposition of cellulose and hemicelluloses were essentially the same in both gases: 0.80 and 0.71, respectively. Of the three wood components, lignin began decomposing at the lowest temperature (110°C). Nevertheless, pyrolysis occurred in an extensive temperature range (up to almost 900°C) at relatively low rates.<sup>8,11</sup> Similar behavior was reported by Mészáros et al.<sup>12</sup> but in the temperature range of 200–600°C. Moreover, the weight-loss profile of lignin depends on the isolation method, the initial degree of condensation,<sup>13</sup> and wood species.<sup>14</sup> Fenner and Lephardt<sup>15</sup> applied Fourier transform infrared/evolved gas analysis to analyze the volatile compounds formed during the thermal decomposition of kraft pine lignin. They established a number of degradation schemes involving various side reactions. Briefly, they noted that the initial degradation of kraft lignin occurred from 120 to 300°C from bond fragmentation in the phenyl propane side chains, as evidenced by the formation of formic acid, formaldehyde, carbon dioxide, water, and sulfur dioxide. The presence of sulfur dioxide supports the argument that sulfur from the kraft pulping process was incorporated into the lignin structure in the form of sulfoxide and/or sulfone linkages. They observed that 50% of the initial weight was lost in the temperature range of 300–480°C at a heating rate of 6°C/min. Methanol, 2-methoxyphenol (guaiacol), and 2-methoxy-4-alkyl-substituted phenol were the most apparent components evolving in this region, indicating fragmentation of the major chain linkages between the monomeric phenol units in the lignin structure.

Fairbridge et al.<sup>16</sup> studied the thermogravimetric behavior of jack pine bark degradation. They noted that the major weight loss began at 180°C. It reached 70% of the initial sample weight. Inorganic ions are known to greatly influence the thermal degradation of polysaccharides<sup>17</sup> as well as lignin.<sup>18</sup> Mészáros et al.<sup>12</sup> associated differences in thermal degradation behavior between wood and bark with the chemical composition in terms of the inorganic ion content. Because bark has significantly higher mineral matter content than wood, bark pyrolysis showed the lowest decomposition temperature.

Fiber degradation during processing may adversely affect the mechanical properties of composites for two main reasons: (1) it changes the fiber structure,

adversely affecting the mechanical properties (namely its resilience), and (2) volatile degradation products usually create microvoids across the interface that act as critical flaws and lead to extensive debonding and failure of the material under service.<sup>19</sup> In addition, natural fiber degradation generally affects the organoleptic properties of wood-based composites, such as odor and color.<sup>20,21</sup> Gonzalez and Myers<sup>22</sup> studied the effect of thermal degradation on the mechanical properties of wood/polymer composites. They observed that, although mechanical properties generally deteriorated as a result of thermal degradation of wood flour, toughness and bending strength were more affected. Wang et al.<sup>20</sup> and Lu et al.<sup>23</sup> suggested a suitable combination of processing variables to limit the thermal degradation of wood fillers. Furthermore, a short compounding time, an appropriate mixing temperature, and a moderate rotation speed improved the compounding quality of modified blends and the dynamic mechanical properties of the resultant composites.<sup>23</sup>

It is well known that the presence of a solid surface in contact with semicrystalline polymers during crystallization from the melt induces heterogeneous nucleation. The process comprises two major events: nucleation and crystal growth.<sup>24–26</sup> For composites based on semicrystalline matrix polymers, crystallinity is an important factor in determining the stiffness and fracture behavior of crystallized matrix polymers.<sup>27</sup> Crystallinity depends on processing parameters such as the crystallization temperature ( $T_c$ ), cooling rate, nucleation density, annealing time, and fiber type.<sup>28,29</sup> As defined by Billon et al.,<sup>30</sup> transcrystallization is a nucleation-controlled process that occurs under quiescent conditions in a semicrystalline polymer in contact with other materials (e.g., fibers). With high heterogeneous nucleation ability of the surface, lateral extension is encumbered, and nucleation growth is therefore strained in one direction, that is, perpendicular to the fiber surface.<sup>28,29</sup> A transcrystalline layer then forms at the fiber/matrix interface. Several researchers have concluded that transcrystalline layer formation improves the interfacial strength and mechanical properties.<sup>31,32</sup> However, no effect or even a negative effect on interfacial and mechanical properties has been reported in other studies.<sup>33</sup> Wang and Liu<sup>28</sup> and Thomason and Van Rooyen<sup>29</sup> found that transcrystallization depends on the fiber type and  $T_c$ . Fiber surface microroughness appears to be an important factor in the morphology of the transcrystalline layer and the ability of the fiber to induce it.<sup>31</sup>

A variety of experimental techniques can be used to investigate the crystallization mechanism under isothermal and nonisothermal conditions. The most common are DSC and optical microscopy.

This work is part of a complete investigation of the effect of wood variability on the properties of

wood–plastic composite materials. The first main objective was to assess the thermal stability of wood during high-density polyethylene (HDPE) melt processing. Thermal sensitivities of various wood types and species were also compared. The second objective was to determine the efficiency of wood fillers as nucleating agents with nonisothermal analysis.

## EXPERIMENTAL

### Materials

Five wood particle types were investigated for thermal stability: eastern white cedar (*Thuja occidentalis*) particles, with sapwood particles and heartwood particles treated separately; jack pine (*Pinus banksiana*) particles, which were divided into wood and bark particles; and black spruce (*Picea mariana*) particles. All lignocellulosic materials were obtained from a softwood sawmill located in Abitibi-Temiscaming in western Quebec, Canada. Wood sawdust and bark shavings were ground in a hammer mill and sieved into several size groups.

For the crystalline investigation, HDPE (Goodfellow Corp., Oakdale, PA) was used as the polyolefin matrix. It is a semicrystalline material (typically 70–80%) with a density of 0.95, a melt index of 9.0 g/10 min, and a melting point of 135°C. An ethylene/maleic anhydride copolymer (MAPE; A-C 575A), supplied by Honeywell (Minneapolis, MN), was used as the coupling agent at a 2 wt % concentration to improve compatibility between the wood filler and thermoplastic matrix. It had a specific gravity of 0.92 and a melting point of 104–107°C.

Wood particles (48–100 mesh) were compounded into pellets at a 45 wt % concentration with HDPE with a Coperion (Stuttgart, Germany) ZSK 25 WLE corotating twin-screw extruder. The barrel temperatures of the four zones were 180, 180, 180, and 190°C from the feeding zone to the die zone. The screw speed was 240 rpm, and vacuum venting (–40 kPa) was applied to minimize volatile extractives. The residence time was 240 s, and the material feed rate was 15 kg/h. Finally, the extrudate was air-cooled and pelletized into pellets with a nominal size of 5 mm. The obtained pellets were used to study the crystallization behavior of HDPE and to assess the nucleating ability of the wood filler.

### Methods

#### TGA

Thermal stability was determined with the standard test method for compositional analysis by thermogravimetry (ASTM E 1131-98). A TA Instruments (New Castle, DE) SDT 2960 simultaneous thermogravimetry/differential thermal analysis apparatus with 0.1- $\mu$ g weight sensitivity was used for the thermogravimetric

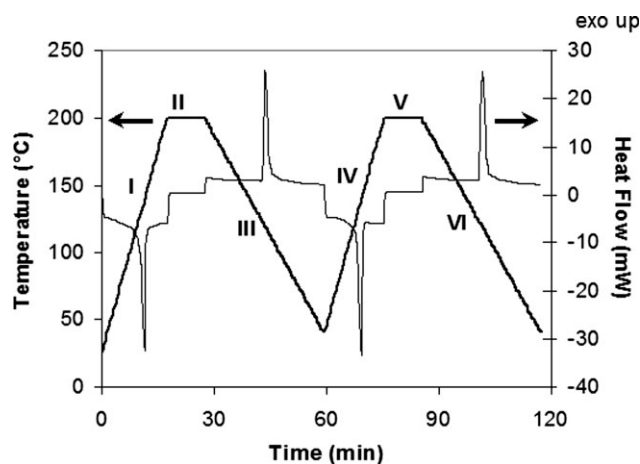


**Figure 1** Thermal program and typical curve of experimental measurements of neat HDPE melting and crystallization.

tests. Samples were tested in a nitrogen environment. Before the measurements, nitrogen was purged for 10 min to establish an inert environment. The sample mass was  $15 \pm 3$  mg. Nonisothermal degradation was then carried out at a 10°C/min heating rate to a final temperature of 600°C.

#### DSC

Crystallization properties were investigated with a Mettler–Toledo DSC 822e differential scanning calorimeter (Mettler–Toledo SAS, Viroflay, France). The thermal program used to determine the melting and crystallization behavior was inspired by the ASTM D 3418-03 standard test method, and it is given in Figure 1. In stage I, samples were heated from room temperature to 200°C at a rate of 10°C/min under a nitrogen atmosphere and held there for 10 min (stage II). In stage III, samples were cooled to room temperature at a cooling rate of 5°C/min. In stage IV, samples were reheated from room temperature to 200°C at a heating rate of 10°C/min and held there for 10 min to destroy any residual nuclei (stage V). Finally, samples were cooled at a cooling rate of 5°C/min (stage VI), during which the crystallization behavior of the composite materials was recorded. A typical curve for the experimental measurements of HDPE melting and crystallization is presented in Figure 1.

If the cooling rate is known, the temperature can be transformed into crystallization time  $t$ , and the relative crystallinity or crystal conversion at time  $t$  [ $\chi_c(t)$ ] can be calculated with the following equation:

$$\chi(t) = \frac{\int_0^t (dH_c/dt) dt}{\int_0^\infty (dH_c/dt) dt} \quad (1)$$

where  $dH_c$  is the enthalpy of crystallization measured during infinitesimal time lapse  $dt$ . The  $t$  and

$\infty$  limits are the elapsed time during and at the end of the crystallization process, respectively. Several parameters from the experimental measurements of DSC exotherms are defined as follows:

- $t_0$  and  $T_0$  are the onset time and onset temperature of crystallization, respectively, measured at the beginning of the primary crystallization stage.
- $t_e$  and  $T_e$  are the time and temperature required for primary crystallization.
- $\Delta t$  (i.e.,  $t_e - t_0$ ) is the broadness of the transition.

The crystallization half-time ( $t_{1/2}$ ), or the time required to convert 50% of the crystallizable material, was obtained from a plot of  $\chi_c(t)$  against  $t$ .  $T_{1/2}$  was the corresponding temperature.

## RESULTS AND DISCUSSION

### Analysis of thermal sensitivity

Weight losses (%) and time derivatives of the weight [differential thermogravimetry (DTG)] in an inert atmosphere are reported in Figure 2 as functions of temperature for the wood and polymer matrix (HDPE).

In agreement with previous findings,<sup>22,34</sup> wood decomposes at lower temperatures than HDPE. The initial weight loss is due to water loss occurring from 60 to 110°C. The thermal decomposition of HDPE can be described by a single-step reaction occurring at 420°C. This simple thermal behavior can be explained by the very homogeneous structure of the thermoplastic, which decomposes in ethylene monomers. On the other hand, wood decomposition curves show two main reaction zones corresponding to (1) devolatilization of materials, with maximum devolatilization rate at about 330–360°C, and (2) decomposition of the produced char, which is characterized by lower rates. The latter will not be considered here because our main objective is to clarify the thermal stability of wood fillers during the melt processing of wood–plastic composites. A clear distinction between these two reaction zones was not possible for bark, most likely because of slower decomposition rates over a broader temperature range of the main components (extractives and lignin). In addition, the main DTG peak corresponds to cellulose decomposition, whereas the shoulder at a lower temperature (ca. 300°C) can be attributed mainly to hemicellulose decomposition.<sup>12</sup> Lignin decomposes at a lower rate in a wide temperature range (200–600°C).<sup>35</sup>

Because the temperature intervals of component decomposition partially overlap, the DTG curves were deconvoluted into four partial curves by an approximation of the experimental curve with mixed

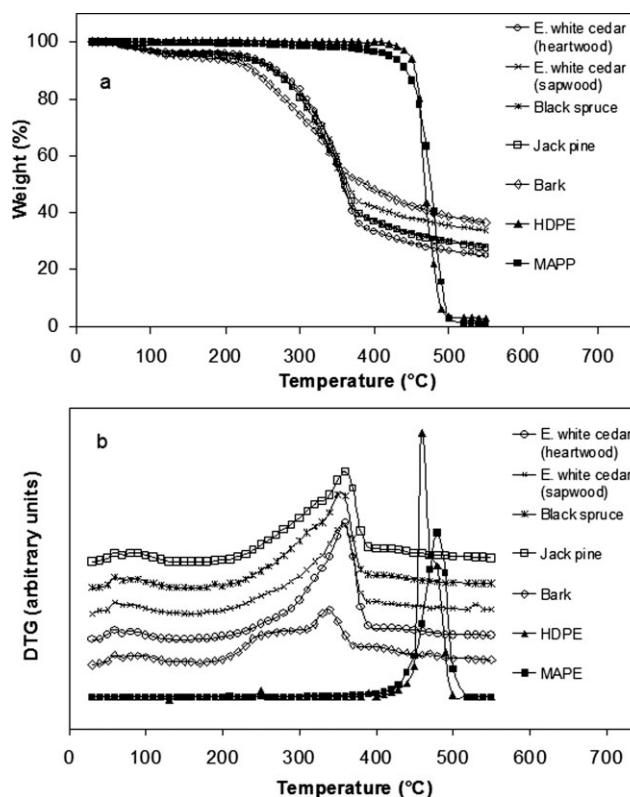


**Figure 2** (a) Weight losses and (b) time derivatives of the weight (DTG) in a nitrogen environment for different wood species and bark.

Lorentzian/Gaussian line shapes corresponding to the degradation of extractives, hemicelluloses, celluloses, and lignin. Corresponding peaks for each region were taken from the literature. Degradation rate characteristics of each component were respected when fitting parameters were defined. For example, lignin starts decomposing at the lowest temperature (110°C) and degrades over an extensive temperature range (up to almost 600°C) at relatively low rates.<sup>8</sup> It was therefore expected that the full width at half-maximum would be very large.

Examples of DTG deconvolution of jack pine wood and bark are shown in Figure 3, whereas Table I summarizes the main characteristic parameters of the regions obtained for the various fillers: the start of extractive, hemicellulose, cellulose, and lignin decomposition is associated with  $T_{e,onset}$ ,  $T_{h,onset}$ ,  $T_{c,onset}$ , and  $T_{l,onset}$ , respectively, whereas the subscript "offset" designates the end of the decomposition process for each component. The peak temperature is indicated by the subscript "peak."

Decomposition is very similar across wood species, and the most remarkable feature is the dissimilarity in DTG characteristics between wood and bark, that is, the decomposition rate around 200°C and the location of peak cellulose decomposition. It is noteworthy that bark decomposition not only



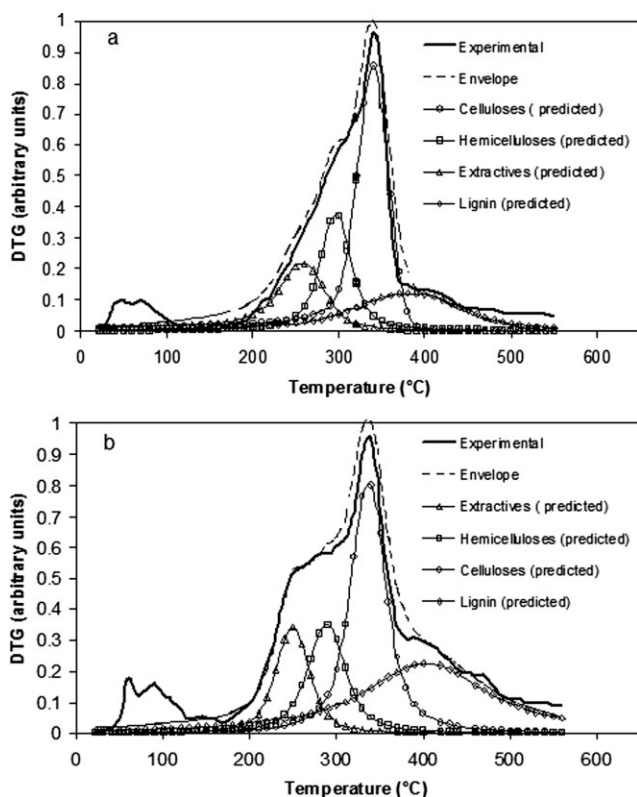


**Figure 3** Global and component decomposition rates for (a) jack pine wood and (b) bark at a heating rate of 10°C/min as measured and predicted by a mixed Lorentzian/Gaussian model.

starts at a lower temperature but also proceeds at a higher rate. This higher bark decomposition rate can be explained by the devolatilization of extractives and the degradation of lignin, both of which are present in greater concentrations in pine bark. Because these compounds are mixtures of a variety of chemical components, they thermally degrade over a large range of temperatures. Furthermore, bark contains a large amount of highly volatile compounds, including alcohols, simple phenolics, fatty

acids, and furans, which are characterized by a higher kinetic devolatilization rate in lower temperature ranges.<sup>36,37</sup> Other findings support the idea that differences in thermal degradation behavior between wood and bark can be attributed to the chemical composition in terms of the inorganic ion content.<sup>38</sup> Because bark has significantly higher mineral matter content than wood, bark pyrolysis shows the lowest decomposition temperature.<sup>12</sup> Branca et al.<sup>36</sup> confirmed that the kinetic degradation of biomaterials depends on the presence of high-molecular-weight components. Hence, an absolute maximum of degradation at high temperatures cannot be achieved with extractives that are less polymerized than cellulose.

Although the DTG peak maximums are in agreement with previous findings, the start of hemicellulose decomposition (onset temperature) and the end of cellulose decomposition (offset temperature) show dissimilarities, mainly because of the deconvolution method. Mészáros et al.<sup>12</sup> determined the onset temperature of hemicellulose decomposition and the offset temperature of cellulose decomposition by extrapolation of the DTG curves. However, their method would be inappropriate in the current study because in most cases, hemicellulose subpeaks are overlapped by cellulose decomposition.

### Crystallinity and nucleating ability analysis

Crystallization parameters obtained from DSC exotherms are summarized in Table II. The values of the crystalline weight fraction [ $\chi_c$ ] were obtained with the following relationship:

$$\chi_c (\%) = \frac{\Delta H_f}{\Delta H_f^0} \times \frac{100}{w} \quad (2)$$

where  $\Delta H_f$  and  $\Delta H_f^0$  are the enthalpy of fusion (DSC endotherm) of the samples and the enthalpy of 100% crystalline HDPE, respectively, and  $w$  is the mass

**TABLE I**  
Thermal Decomposition Parameters of the Wood Components

Component	Temperature (°C)	Eastern white cedar (sapwood)	Eastern white cedar (heartwood)	Jack pine	Black spruce	Bark (jack pine)
Extractives	$T_{e,onset}$	174	178	171	168	183
	$T_{e,peak}$	254	251	260	254	250
	$T_{e,offset}$	348	351	350	346	340
Hemicelluloses	$T_{h,onset}$	198	201	196	196	200
	$T_{h,peak}$	291	293	298	302	292
	$T_{h,offset}$	382	384	382	386	390
Celluloses	$T_{c,onset}$	281	282	284	278	255
	$T_{c,peak}$	363	361	360	362	338
	$T_{c,offset}$	428	430	423	431	470
Lignin	$T_{l,onset}$	115	115	112	110	115
	$T_{l,peak}$	397	392	391	394	407
	$T_{l,offset}$	>600	>600	>600	>600	>600
Decomposition rate around 200°C (%/min)		0.25	0.22	0.21	0.18	0.46

**TABLE II**  
**Nonisothermal Parameters for HDPE and Various Wood Particle/HDPE Composites Determined from DSC Exotherms**

Crystallization parameter	Neat HDPE	HDPE/jack pine	HDPE/black spruce	HDPE/eastern white cedar	HDPE/bark
$T_0$ (°C)	119.60	122.73	122.19	122.05	122.32
$t_0$ (min)	6.27	5.47	5.64	5.68	5.57
$T_c$ (°C)	115.70	119.63	121.01	120.61	120.87
$t_c$ (min)	6.94	6.26	5.97	6.05	6.22
$T_e$ (°C)	108.27	113.69	115.13	113.87	115.06
$t_e$ (min)	8.35	7.12	7.04	7.27	7.05
$\Delta t_c$ (min)	2.08	1.65	1.4	1.59	1.48
$T_{1/2}$ (°C)	112.49	117.80	118.75	118.09	118.57
$t_{1/2}$ (min)	7.53	6.6	6.45	6.47	6.55
$\chi_c$ (%)	75.59	77.36	76.15	75.97	74.60

fraction of HDPE in the composite. DSC analysis of pure HDPE reveals a relatively high crystallinity (217.69 J/g or 75.59% crystallinity if the enthalpy of 100% crystalline polyethylene is taken to be 288 J/g<sup>39</sup>). Figure 4 depicts the crystallization exotherms of HDPE and its various blends at a cooling rate of 5°C/min. The overall crystallization process of a semicrystalline polymer is usually divided into two main phases: primary crystallization and secondary crystallization. Primary crystallization is the macroscopic expansion of the degree of crystallinity as a result of two consecutive microscopic mechanisms: nucleation and subsequent crystal growth. Secondary crystallization mainly involves the crystallization of lateral and interfibrillar chains.

As depicted in Figure 4, all obtained exotherms show a dominant sharp exothermic peak at higher temperatures, which is followed by a shallow tail at lower temperatures. According to Figure 4 and Table II, the addition of wood particles to HDPE results in an increase in  $T_c$  and  $\chi_c$  of the HDPE matrix. This is due to the nucleating ability of wood particles in the crystallization of HDPE. In fact, during nonisothermal crystallization, the heterogeneous nucleation activity of wood shifts the DSC exothermic peak to-

ward a higher temperature, depending on the wood particle type. The highest increase in  $T_c$  ( $\approx 6^\circ\text{C}$ ) was found with the HDPE/black spruce wood particle composites in comparison with neat HDPE, and the lowest increase was observed with HDPE/jack pine composites. Consequently, it can be argued that wood particles act as heterogeneous nucleation agents for HDPE. Moreover, Table II shows that the crystallinity of pure HDPE is slightly increased by the addition of wood particles.

The highest crystallinity was obtained with HDPE/jack pine composites (77.4%). However, the effect is not clear when bark particles are added. Similar findings have been reported by many researchers. Joseph et al.<sup>27</sup> observed an increase in the crystallinity and  $T_c$  after the addition of sisal fibers to a polypropylene matrix. Recently, Borysiak<sup>40</sup> reported a strong increase in  $T_c$  (5–9°C) when pine or beech wood fibers were added to a polypropylene matrix. Furthermore, it has been reported that the crystallinity and  $T_c$  of the polymer phase is further increased by filler content.<sup>41</sup>

The overall crystallization time ( $\Delta t_c$ ) of HDPE decreased with the addition of wood particles, from 2.08 min for neat HDPE to 1.65 min for HDPE/jack

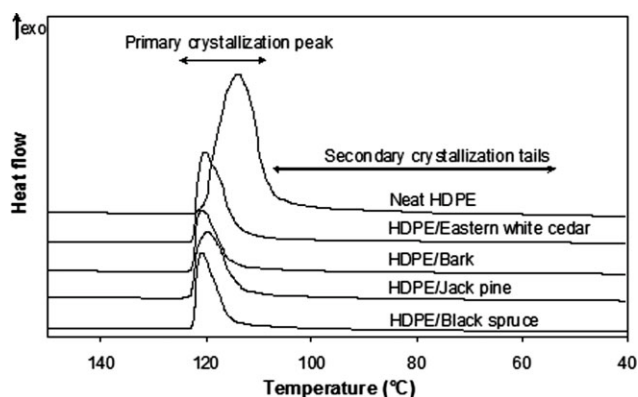


**Figure 4** Crystallization exotherms of HDPE and its blends at a cooling rate of 5°C/min.

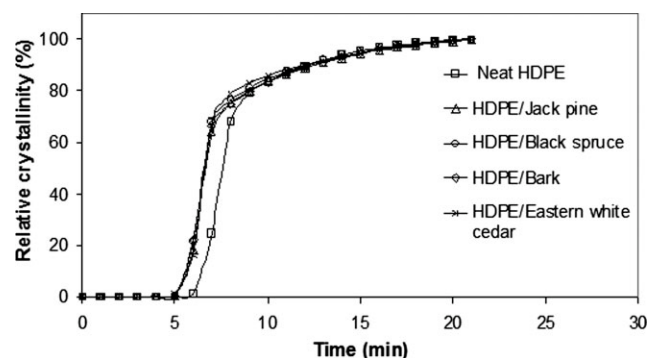


**Figure 5** Relative crystal conversion of the HDPE polymer and its corresponding blends.

pine particles, and reached 1.4 min when black spruce particles were added.

The presence of wood particles affects not only the degree of HDPE crystallinity but also the crystal conversion kinetics. Figure 5 shows the variation in the measured crystal conversion of HDPE with various wood fillers. All the crystal conversion curves have a similar sigmoidal shape. The curvature tails in the upper part of the plot are due to the secondary phase of the crystallization process. Differences in the crystal conversion kinetics between pure HDPE and its blends are evident during the primary stage of the crystallization process only: crystal conversion increases for HDPE filled with wood particles. This can also be explained by the nucleating ability of wood particles. However, the wood particles show similar effects on crystal conversion, and the differences in the crystal conversion values are insufficient to allow adequate discrimination between composites.

$t_{1/2}$  of HDPE, a useful parameter for comparing the nucleating ability of wood fillers, decreases in comparison with that of pure HDPE (Table II). The decline in  $t_{1/2}$  has been estimated to be around 1 min, depending on the wood type. Borysiak<sup>40</sup> concluded that the lower the  $t_{1/2}$  values are, the higher the nucleating efficiency is.

In summary, it can be concluded that the nucleation ability is improved when wood particles are added to the HDPE matrix. The nucleating efficiency of a filler is considered a critical factor in polymer processing. Composite materials with high nucleating ability require a shorter injection-molding time.<sup>40</sup> Although previous findings are generally in good agreement with our results, a few reports differ. Mucha and Krölikowski<sup>42</sup> compared the nucleating efficiency of various organic (wood flour and chitosan) and inorganic (carbon black and nanoclay particles) fillers in isotactic polypropylene (iPP). They concluded that the presence of chitosan or wood flour hinders the diffusion of iPP macromolecules in the crystallization process and disrupts the creation of the iPP spherulitic structure. Consequently, further investigations are needed to clarify the role of wood surface chemistry in the nucleation activity and crystallization kinetics of polymers. Moreover, it is widely known that polymer nucleation in the presence of substrates is not straightforward; it requires a thorough knowledge of the chemical composition and topography of the surface filler. Mathew et al.<sup>43</sup> examined how the size, chemical composition, and surface topography of cellulosic materials (microcrystalline cellulose, cellulose fibers, and wood flour) affect poly(lactic acid) crystallization. Using DSC and optical microscopy, they found that microcrystalline cellulose and wood flour had better nucleating ability than cellulose fibers. On the

other hand, Borysiak and Doczekalska<sup>44</sup> reported that the crystal conversion of iPP was highly altered by a chemical treatment of the filler surface, with potential consequences for the wood's nucleation ability. Their observations indicated that improved interaction between the pine wood and polymeric matrix caused a decrease in the nucleation properties of fillers and iPP crystallization.

## CONCLUSIONS

The main devolatilization stage of wood fillers occurs at temperatures lower than that of HDPE. Compared to the decomposition of wood, bark decomposition begins at a lower temperature and is processed at a higher rate. Dissimilarities between wood and bark thermal decomposition have been attributed to higher extractive, lignin, and inorganic ion contents. Consequently, the HDPE melt process influences bark filler decomposition more than wood filler decomposition.

The nucleating activity for various wood fillers has been evaluated with  $\chi_c$ ,  $t_{1/2}$ , and  $T_c$  of the HDPE matrix. The nucleation ability has been improved by the addition of wood particles to the HDPE matrix. Wood particles have shown only a slight effect on crystal conversion, and the differences in crystal conversion were insufficient to adequately discriminate between the composites. Finally, given the ambiguity in the nature of the interaction between the polymer and the wood surfaces, which determines the orientation of crystalline HDPE, further investigations are recommended, mainly with X-ray diffraction (wide-angle X-ray diffraction and small-angle X-ray scattering).

The authors are grateful to A. Adnot for scientific contributions.

## References

1. Placet, V.; Passard, J.; Perré, P. *J Mater Sci* 2008, 43, 3210.
2. Hillis, W. E. *Wood Sci Technol* 1984, 18, 281.
3. Ngula Inari, G.; Petrissans, M.; Lambert, J.; Ehrhardt, J. J.; Gérardin, P. *Surf Interface Anal* 2006, 38, 1336.
4. Chow, S. Z. *Wood Sci Technol* 1971, 5, 27.
5. Tjeerdsma, B. F.; Militz, H. *Holz Roh Werkstoff* 2005, 63, 102.
6. Christiansen, A. W. *Wood Fiber Sci* 1990, 22, 441.
7. Sernek, M.; Kamke, F. A.; Glasser, W. G. *Holzforschung* 2004, 58, 22.
8. Ramiah, M. V. *J Appl Polym Sci* 1970, 14, 1323.
9. Müller-Hagedorn, M.; Bockhorn, H.; Krebs, L.; Müller, U. *J Anal Appl Pyrolysis* 2003, 68, 231.
10. Rath, J.; Wolfinger, M. G.; Steiner, G.; Krammer, G.; Barontini, F.; Cozzani, V. *Fuel* 2003, 82, 81.
11. Orfão, J. J. M.; Antunes, F. J. A.; Figueiredo, J. L. *Fuel* 1999, 78, 349.
12. Mészáros, E.; Jakab, E.; Várhegyi, G.; Szepesváry, P.; Marosvölgyi, B. *J Anal Appl Pyrolysis* 2004, 72, 317.

13. Gardner, D. J.; Schultz, T. P.; McGinnis, G. D. *J Wood Chem Technol* 1985, 5, 85.
14. Faix, O.; Jakab, E.; Till, F.; Székely, T. *Wood Sci Technol* 1988, 22, 323.
15. Fenner, R. A.; Lephardt, J. O. *J Agric Food Chem* 1981, 29, 846.
16. Fairbridge, C.; Ross, R. A.; Spooner, P. *Wood Sci Technol* 1975, 9, 257.
17. DeGroot, W. F.; Shafizadeh, F. *J Anal Appl Pyrolysis* 1984, 6, 217.
18. Jakab, E.; Faix, O.; Till, F.; Székely, T. *J Anal Appl Pyrolysis* 1993, 25, 185.
19. Nabi Saheb, D.; Jog, J. P. *Adv Polym Technol* 2000, 19, 41.
20. Wang, Y.; Chan, H. C.; Lai, S. M.; Shen, H. F. *Int Polym Process* 2001, 16, 100.
21. Nabi Saheb, D.; Jog, J. P. *Adv Polym Technol* 1999, 18, 351.
22. Gonzalez, C.; Myers, G. E. *Int J Polym Mater* 1993, 23, 67.
23. Lu, J. Z.; Wu, Q.; Negulescu, I. I. *J Appl Polym Sci* 2004, 93, 2570.
24. Avrami, M. *J Chem Phys* 1939, 7, 1103.
25. Avrami, M. *J Chem Phys* 1940, 8, 212.
26. Avrami, M. *J Chem Phys* 1941, 9, 177.
27. Joseph, P. V.; Joseph, K.; Thomas, S.; Pillai, C. K. S.; Prasad, V. S.; Groeninckx, G.; Sarkissova, M. *Compos A* 2003, 34, 253.
28. Wang, C.; Liu, C. R. *Polymer* 1999, 40, 289.
29. Thomason, J. L.; Van Rooyen, A. A. *J Mater Sci* 1992, 27, 889.
30. Billon, N.; Henaff, V.; Haudin, J. M. *J Appl Polym Sci* 2002, 86, 734.
31. Zafeiropoulos, N. E.; Baillie, C. A.; Matthews, F. L. *Compos A* 2001, 32, 525.
32. Zhang, M.; Xu, J.; Zhang, Z.; Zeng, H.; Xiong, X. *Polymer* 1996, 37, 5151.
33. Wang, C.; Hwang, L. M. *J Polym Sci Part B: Polym Phys* 1996, 34, 1435.
34. Wielage, B.; Lampke, T.; Marx, G.; Nestler, K.; Starke, D. *Thermochim Acta* 1999, 337, 169.
35. Jakab, E.; Faix, O.; Till, F. *J Anal Appl Pyrolysis* 1997, 40, 171.
36. Branca, C.; Di Blasi, C.; Elefante, R. *Energy Fuels* 2006, 20, 2253.
37. Shafizadeh, T. In *Progress in Biomass Conversion*; Sarkanen, K. V., Tillman, D. A., Eds.; Academic Press: New York, 1981.
38. Hosoya, T.; Kawamoto, H.; Saka, S. *J Wood Sci* 2007, 53, 351.
39. Wunderlich, B. *Macromolecular Physics II*; Academic: New York, 1973.
40. Borysiak, S. *J Therm Anal Calorim* 2007, 88, 455.
41. Joseph, P. V.; Joseph, K.; Thomas, S. *Compos Sci Technol* 1999, 59, 1625.
42. Mucha, M.; Królikowski, Z. *Wpływ Napeniaczy Kinet Krystal Polipropylenu* 2004, 25, 1373.
43. Mathew, A. P.; Oksman, K.; Sain, M. *J Appl Polym Sci* 2006, 101, 300.
44. Borysiak, S.; Doczekalska, B. *Holz Roh Werkstoff* 2006, 64, 451.